

PERSPECTIVE | APRIL 15 2024

Nano-kirigami/origami fabrications and optical applications

SCI F FREE

Yingying Chen ; Xiaowei Li ; Lan Jiang ; Yang Wang  ; Jiafang Li  



Appl. Phys. Lett. 124, 160501 (2024)

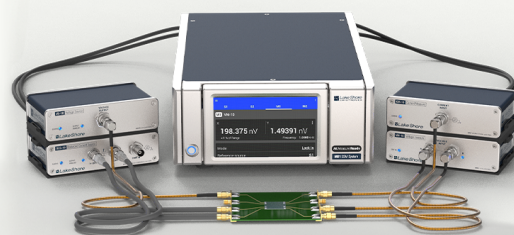
<https://doi.org/10.1063/5.0199052>



An innovative I-V characterization system for next-gen semiconductor R&D

Unique combination of ultra-low noise sourcing + high-sensitivity lock-in measuring capabilities

[Learn more](#)



Nano-kirigami/origami fabrications and optical applications

Cite as: Appl. Phys. Lett. **124**, 160501 (2024); doi: [10.1063/5.0199052](https://doi.org/10.1063/5.0199052)

Submitted: 21 January 2024 · Accepted: 14 March 2024 ·

Published Online: 15 April 2024



View Online



Export Citation



CrossMark

Yingying Chen,¹ Xiaowei Li,² Lan Jiang,² Yang Wang,^{1,a)} and Jiafang Li^{1,3,a)}

AFFILIATIONS

¹Key Lab of Advanced Optoelectronic Quantum Architecture and Measurement (Ministry of Education), Beijing Key Lab of Nanophotonics and Ultrafine Optoelectronic Systems, and School of Physics, Beijing Institute of Technology, Beijing 100081, China

²Laser Micro/Nano Fabrication Laboratory, School of Mechanical Engineering, Beijing Institute of Technology, Beijing 100081, China

³BIT Chongqing Institute of Microelectronics and Microsystem, Chongqing 400000, China

^{a)}Authors to whom correspondence should be addressed: yangwang@bit.edu.cn and jiafangli@bit.edu.cn

ABSTRACT

Emerging nano-kirigami/origami technology enables the flexible transformations of 2D planar patterns into exquisite 3D structures *in situ* and has aroused great interest in the areas of nanophotonics and optoelectronics. This paper briefly reviews some milestone research and breakthrough progresses in nano-kirigami/origami from the aspects of stimuli approaches and application directions. Versatile stimuli for kirigami/origami, including capillary force, residual stress, mechanical force, and irradiation-induced stress, are introduced in the micro/nanoscale region. Appealing optical applications and reconfigurable schemes of nano-kirigami/origami structures are summarized, offering effective routes to realize tunable nanophotonic and optoelectronic devices. Future challenges and promising pathways are also envisioned, including design methods, innovative materials, multi-physics field driving, and reprogrammable devices.

Published under an exclusive license by AIP Publishing. <https://doi.org/10.1063/5.0199052>

I. INTRODUCTION

Over the past decade, kirigami/origami technology, a combination of paper-cuts like patterning and transforming processes, has gained widespread recognition across various fields, such as mechanics, biology, medicine, microelectronics, acoustics, optics, etc., all thanks to their magical geometric transformations.^{1–9} Especially, with the development of materials and high-precision fabrication techniques, kirigami/origami principle has been rapidly applied in micro/nanoscale,^{10–18} since it enables the direct transformations of two-dimensional (2D) micro/nanoscale materials/structures into three-dimensional (3D) structures without the need of precise splicing. Benefited from the tiny scales that are comparable to optical wavelengths, the resulted structures exhibited extraordinary performances in terms of continuity, complexity, optical resonances, geometric evolution, and dynamic modulation.^{2,19} Therefore, the realization of micro/nanoscale kirigami/origami has aroused great interest, and various actuation methods were developed, including capillary forces,^{20–22} residual stress,^{23,24} mechanical stress,^{12,25,26} and focused-ion-beam (FIB) irradiation-induced stress,^{27–31} depending on different environments and materials. Especially, with the FIB-based *in situ* transformation

method demonstrated in 2018, the concept of kirigami/origami in micro/nanoscale (named nano-kirigami/origami) has been well established and gradually evolved into a distinctive frontier research area.

In this paper, we present a brief overview of the research progresses in the emerging nano-kirigami/origami area. Specifically, Sec. II introduces the typical kirigami/origami strategies based on various stimuli methods, in which the advancements and principles of FIB-based 3D nano-kirigami method are highlighted. In Sec. III, a broad picture is outlined with diverse applications of 3D nano-kirigami/origami structures, including optical chirality, polarization conversion, Fano resonance generation, phase modulation, thermal management, and reconfigurable optoelectronic devices. These achievements provide an appealing platform and research methodology for the development of multifunctional 3D nanostructures, optoelectronic devices, micro/nano-electromechanical systems (MEMS/NEMS), and strain-based photonic materials. Finally, conclusions and outlooks are presented in Sec. IV, where the challenges and potential directions of nano-kirigami/origami are envisioned from the aspects of structural design methods, innovative materials, multi-physics field driving, and reprogrammable optical devices.

II. ADVANCEMENTS IN ACTUATION METHODS

A. Typical kirigami/origami strategies

Figure 1 illustrates the multi-physics field driving schemes of micro-/nano-kirigami, including mechanical, thermal, acoustic, optical, electric, and magnetic methods.^{32–38} Among them, the mechanical force is one of the most common stimuli in nature that can trigger geometric transformations. Capillary forces and film residual stresses, as two typical surface tension forces in mechanics, have been widely adopted in 3D structure deformations. For example, as the thin film based residual stress illustrated in Fig. 2(a), when the sacrificial layer at the bottom is removed by etching or other methods, the overhanging structure will undergo self-curling deformation due to residual stresses. With this principle, Mei *et al.* fabricated versatile coiled tubes, of which the diameters and lengths could be precisely tuned, integrated, and functionalized by releasing and rolling up the SiO/SiO₂ nanofilms,³⁹ as shown in Fig. 2(b). Meanwhile, Chalapat *et al.* used reactive ion etching (RIE) to fabricate 3D metal flowers (cages) on Ti/Al/Cr thin film in Fig. 2(c).²⁹ Liu *et al.* described a fast, high-curvature, reconfigurable 3D origami structure that is driven by the strain generated by electrochemical reactions on the surface of Pt,⁴⁰ as plotted in Figs. 2(d) and 2(e).

Mechanically guided assembly force is another effective approach to directly and accurately control the deformation mode and degree on demand. In this strategy, the designed 2D precursor is partially fixed on the pre-stretched planar substrate. When the substrate is released, its deformation drives the movements of the binding site connected to the structure, resulting in mechanical compression force to make the structure buckle and deform, as shown in Fig. 2(f). Such principle can be implemented in a wide range from millimeters to 10 nm, as shown in Fig. 2(g).²⁶

FIB-irradiation-induced force, by taking advantage of the advanced semiconductor technology, provides an exceptional approach to achieve miniature and *in situ* structural deformations.^{41,42} By accurately milling and folding suspended nanomembranes with accelerated ion beams, the structures can be folded, bent, and twisted in micro/nanoscale, making FIB an ideal tool for nano-kirigami.³⁰ However, at the initial stage, the 3D fabricated structures were mainly based on rigid folding in one or multiple processes,^{27,31,43,44} as shown in Fig. 2(i). From the topological perspective, such geometries are relatively simple and belong to the tree-type (open-loop) design, i.e., the deformation parts of the structure are independent of each other, which greatly limits the flexibility of the overall deformation effect of the structure.^{19,31}

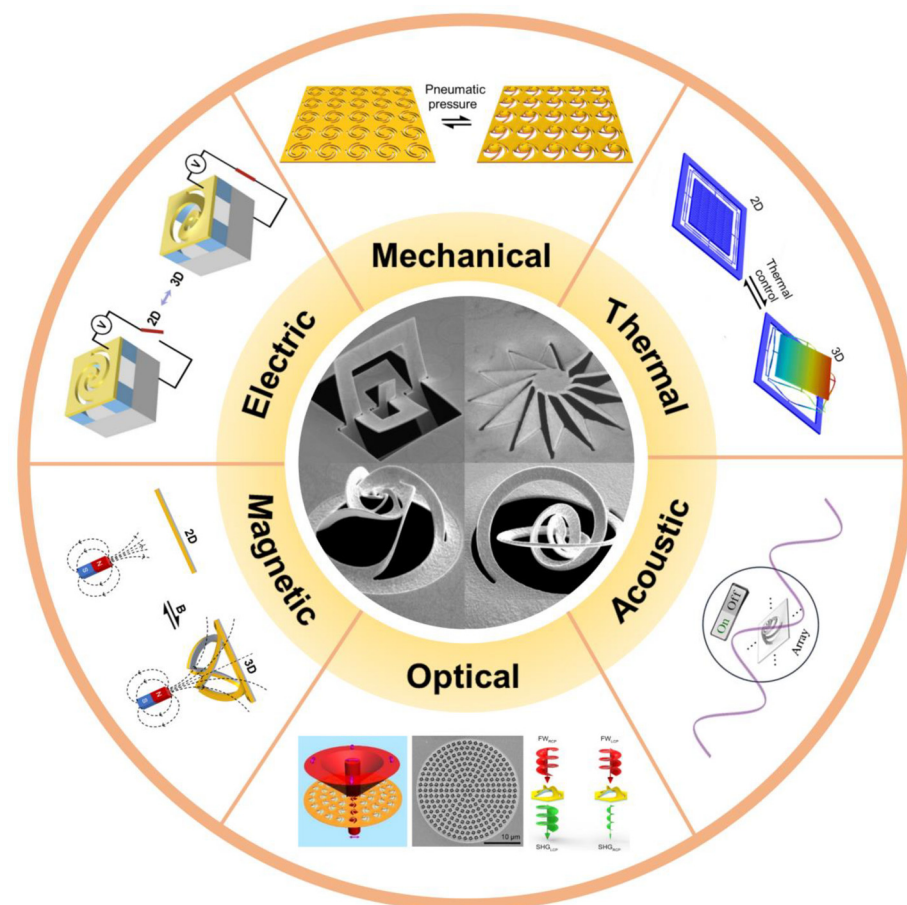


FIG. 1. Overview of nano-kirigami/origami multi-physics field driving schemes. Inner circle: various nano-kirigami/origami structures. Outer circle: nano-kirigami/origami multi-physics field driving schemes, covering mechanical,³² thermal,³⁴ acoustic,³⁷ optical,^{38,39} magnetic,³³ and electric³⁵ driving approaches. Reproduced with permission from Chen *et al.*, *Photonics Res.* **8**(7), 1177–1182 (2020). Copyright 2020 OSA.³² Reproduced with permission from Zhao *et al.*, *J. Opt.* **24**, 054007 (2022). Copyright 2022 IOP Publishing.³⁴ Reproduced with permission from Cao *et al.*, *Phys. Rev. Appl.* **18**, 054040 (2022). Copyright 2022 APS.³⁷ Reproduced with permission from Liu *et al.*, *APL Photonics* **3**, 100803 (2018). Copyright 2018 AIP Publishing.³⁸ Reproduced with permission from Tang *et al.*, *Laser Photonics Rev.* **14**(7), 2000085 (2020). Copyright 2020 Wiley.³⁹ Reproduced with permission from Chen *et al.*, *J. Appl. Phys.* **131**, 233102 (2022). Copyright 2022 AIP Publishing.³³ Reproduced with permission from Chen *et al.*, *Nat. Commun.* **12**(1), 1299 (2021). Copyright 2021 Springer Nature.³⁵

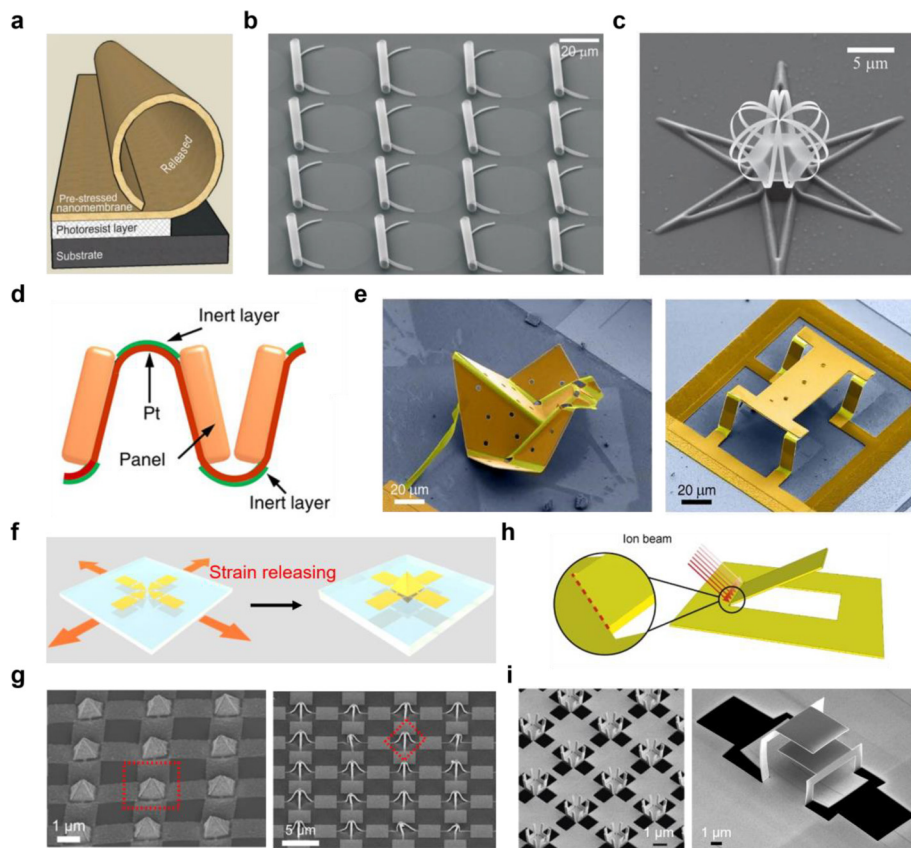


FIG. 2. Typical 3D kirigami/origami strategies. (a) Schematic illustrations of residual stress.³⁹ (b) Rolled-up nanomembranes.³⁹ (c) Reactive ion etching (RIE) induced plastic strain.²⁹ (d) Schematic of a bidirectionally folded surface electrochemical actuator (SEA).⁴⁰ (e) SEA-enabled microscale origami structures.⁴⁰ (f) Schematic illustration of the strain release-induced force.²⁶ (g) Mechanically assembled structures formed by releasing a biaxially deformed polydimethylsiloxane (PDMS) substrate.²⁶ (h) Schematic illustration of FIB-induced folding scheme.²⁷ (i) Local FIB irradiation induced folding of boxes with U-shaped walls and a triple-layer structure.^{27,31} (a) and (b) Reproduced with permission from Mei *et al.*, *Adv. Mater.* **20**(21), 4085–4090 (2008). Copyright 2008 Wiley.³⁹ (c) Reproduced with permission from Chalapat *et al.*, *Adv. Mater.* **25**(1), 91–95 (2013). Copyright 2013 Wiley.²³ (d) and (e) Reproduced with permission from Liu *et al.*, *Sci. Rob.* **6**, eabe6663 (2021). Copyright 2021 AAAS.⁴⁰ (f) and (g) Reproduced with permission from Liu *et al.*, *ACS Nano* **13**(1), 440–448 (2019). Copyright 2019 ACS.²⁶ (h) and (i) Reproduced with permission from Cui *et al.*, *Light* **4**(7), e308 (2015). Copyright 2015 CIOMP.²⁷ Reproduced with permission from Li *et al.*, *Nanophotonics* **7**(10), 1637–1650 (2018). Copyright 2018 De Gruyter.³¹

B. Nano-kirigami based on FIB irradiation

To address the limitations, we proposed a type of close-loop geometric patterns in 2018, by using high-dose FIB to mill self-supported gold nanofilms and low-dose FIB for global irradiation to realize 3D nanostructure deformation.³⁰ It was found that versatile *in situ* folding, buckling, rotation, and distortion can be achieved during the continuous 3D deformation process and could reach the similar characteristics as their macroscopic counterparts (this is actually the origin of the word “nano-kirigami.”) With the help of a bilayer stress model³⁰ illustrated in Figs. 3(a)–3(c), complex 3D nano-kirigami structures, in mimicking their macroscopic paper-cuts by a downscaling of 1/10 000, were readily simulated and realized, as shown in Figs. 3(d) and 3(e). Specifically, when the gold nanofilm is irradiated by ion beams, some gold atoms are knocked out and cause surrounding atoms to aggregate toward the vacancies, resulting in tensile stress close to the surface of the film, as shown in Fig. 3(a). Meanwhile, the inner atoms are subjected to compressive stress due to the influence of implanted gallium ions. These two types of stresses occur within a thickness of ~ 20 nm on the top layer of the gold film, which further drives the elastic deformation of bottom layer.³¹ Therefore, the physical phenomena caused by the nano-kirigami method can be simplified into a bilayer stress model in Fig. 3(b), i.e., the top layer with tensile stress (dominant stress) and the bottom layer with deformation stress. Figure 3(c) shows two typical upward or downward bending structural deformations,

when one or both ends of the cantilever are fixed, respectively. One advantage of such nano-kirigami method is that the structural geometries are highly flexible and extendable in both in-plane and out-of-plane dimensions,^{30,45} as shown in Figs. 3(f)–3(i), providing a reliable and flexible research platform for the design and application of micro/nanostructures with exotic geometries.

III. APPLICATIONS

Compared with its macroscopic counterpart, the uniqueness of nano-kirigami/origami is that the structural size is close to or smaller than optical wavelengths and can be arranged in an array, which are highly preferable for the generation of local and collective optical resonances, respectively. Nano-kirigami/origami can enable versatile 2D-to-3D shape transformation and result in unique applications in modulating the mechanical, electrical, magnetic, and optical properties of existing materials, with remarkable deformation flexibility, structural diversity, functionality, generality, reconfigurability, and on-chip integrability. These important characteristics have been applied for the generation of versatile optical functionalities, such as optical chirality, polarization conversion, Fano resonance generation, phase modulation, thermal management, and reconfigurable optoelectronic devices, providing an outstanding platform for the development of nanophotonic and optoelectronic devices, MEMS/NEMS, strain-based photonic materials, etc.

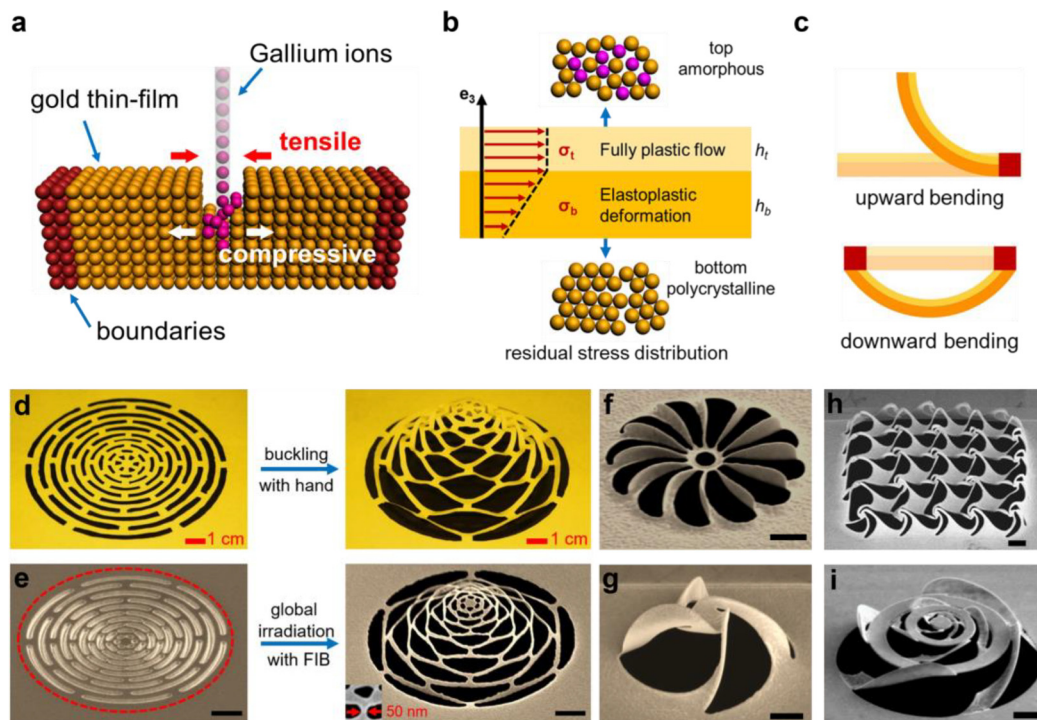


FIG. 3. Nano-kirigami based on FIB irradiation. (a) Residual stress distribution of self-supported nano-gold films under FIB irradiation.³⁰ (b) Bilayer stress distribution model.³⁰ (c) A diagram of two typical structural deformations (up and down bending) when one or both ends of a suspended structure are fixed (indicated by red squares).³¹ (d) Camera images of paper kirigami and (e) SEM images of close-loop nano-kirigami of an expandable dome.³⁰ Scale bars: 1 μm . (f)–(i) 3D close-loop nano-kirigami structures fabricated by FIB.^{30,45} Scale bars: 1 μm . (a) and (b) and (d)–(h) Reproduced with permission from Liu *et al.*, *Sci. Adv.* 4, eaat4436 (2018).³⁰ Copyright 2018 AAAS. (c) Reproduced with permission from Li *et al.*, *Nanophotonics* 7(10), 1637–1650 (2018). Copyright 2018 De Gruyter.³¹ (i) Reproduced with permission from Han *et al.*, *Photonics Res.* 8(9), 1506–1511 (2020). Copyright 2020 OSA.⁴⁵

A. Optical chirality and polarization conversion

Compared with macroscopic kirigami/origami and the 2D planar devices fabricated by other 3D nanofabrication methods, one important feature of nano-kirigami is that the 3D twisted structures fabricated by FIB-irradiation break the 2D mirror symmetry in the nanoscale and can support optical chiral responses when interacting with circularly polarized light.^{30,46} For example, for the nano-kirigami pinwheel arrays in Fig. 4(a),³⁰ it was found that the 2D pinwheel structures did not have any chiral response, while the 3D pinwheel structures not only have obvious circular dichroism (CD) responses but also exhibited very strong circular birefringence (CB) characteristics, as plotted in Figs. 4(b) and 4(c). Such experimental observations, as well as numerical simulations, unambiguously demonstrated the exceptional optical functionalities of nano-kirigami structures.

In addition to the chiroptical responses, the diffractive polarization conversion effect was also observed in nano-kirigami metasurfaces.³⁶ As presented in Fig. 4(d), when the x-polarized light is incident on the 3D pinwheel array with alternating LH and RH arrangement, the transmitted y-polarized light at certain wavelength region (1.6 μm) experiences a π phase difference, based on which a diffraction grating is formed in Fig. 4(e). As a result, the grating structure exhibits a strong diffractive polarization conversion characteristic at $\lambda = 1.6 \mu\text{m}$, as shown in Fig. 4(f), where the measured y-polarized light is diffractively separated from the original x-polarized incident light along the incident direction.

The lattice effect is another uniqueness of the nano-kirigami array compared to its macroscopic counterpart. For example, counterintuitive sign reversal of CD without changing the geometric chirality was achieved by simply constructing an array of twisted propeller-like chiral metamolecules.^{47,48} The underlying principle is to tailor the coupling between the intracellular and intercellular units by rotating the propeller metamolecule blade with an angle of φ . As shown in Fig. 4(g), when φ decreases from 35° to 7.5° , the maximum CD value of the metamolecule structure changes from 0.46 to -0.58 , obtaining a drastic CD reversal. This concept and configuration of artificial propeller pave a useful way for the study on chiral physics and provide a valuable platform for the development of chiral materials. Moreover, a bionic nano-cilia metasurface array with enhanced CD was realized in the visible wavelength band,⁴⁹ offering an inspirational sensing scheme for neurology and biology.

B. Fano resonance generation

Compared with the 2D metasurfaces fabricated by other nanofabrication methods, nano-kirigami structures fabricated by FIB-irradiation naturally have both out-of-plane stereo elements and in-plane arrays, which are favorable for the generation of surface lattice resonances and Fano resonances. Traditionally, Fano resonance is generated by the coherent coupling of continuous and discrete state levels,⁵⁰ with particularly sharp and asymmetric line shape, which has

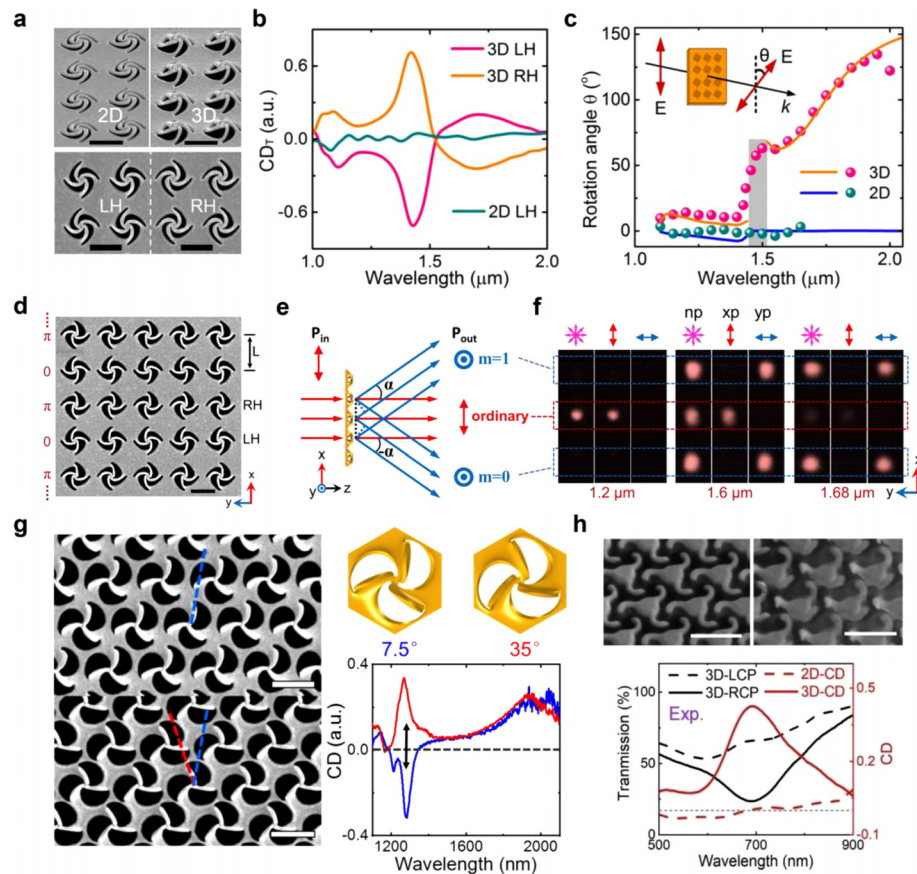


FIG. 4. Applications in optical chirality and polarization conversion. (a) SEM images of left-handed (LH) and right-handed (RH) pinwheel structures.³⁰ Scale bars: 1 μm . (b) CD spectra of 2D LH, 3D LH, and 3D RH pinwheel structures.³⁰ (c) Experimental (dot) and calculated (solid line) comparison of the relation between rotation angle θ and incident wavelength under linearly polarized incidence.³⁰ (d) Top-view SEM image of the linear grating of alternately arranged LH and RH pinwheels.³⁶ Scale bar: 1 μm . (e) Schematic of the linear grating for polarization modulation at x-polarized incidence.⁴⁶ (f) CCD camera images of the transmitted light spots at $\lambda = 1.20$, 1.60, and 1.68 μm , respectively, under detection with no polarization (np), x-polarization (xp), and y-polarization (yp).³⁶ (g) SEM images and measured CD spectra of the two bi-chiral propeller metamolecule arrays in which the rotating angles (ϕ) of the blades are 7.5° and 35°, respectively.⁴⁸ Scale bars: 1 μm . (h) Side-view SEM images and measured CD spectra of 2D and 3D deformed nano-cilia metasurfaces.⁴⁹ Scale bars: 500 nm. (a)–(c) Reproduced with permission from Liu *et al.*, *Sci. Adv.* 4, eaat4436 (2018). Copyright 2018 AAAS.³⁰ (d)–(f) Reproduced with permission from Liu *et al.*, *APL Photonics* 3, 100803 (2018). Copyright 2018 AIP Publishing.³⁶ (g) Reproduced with permission from Li *et al.*, *Adv. Opt. Mater.* 9(24), 2101191 (2021). Copyright 2021 Wiley.⁴⁸ (h) Reproduced with permission from Liu *et al.*, *Nanophotonics* 12(8), 1459–1468 (2023). Copyright 2023 De Gruyter.⁴⁹

been widely observed from atomic systems to photonic crystals, metamaterials, and other plasma systems.^{51,52} The couplings between out-of-plane local resonance and in-plane lattice resonance of nano-kirigami metasurfaces provide an ideal pathway for the generation of Fano resonances.^{53–56} For example, metamaterials composed of vertical asymmetric split ring resonators (aSRRs) can exhibit dramatic triple Fano resonances in the near infrared wavelengths based on a 3D conductive coupling mechanism,⁵⁵ as shown in Figs. 5(a) and 5(b). This strategy provides a useful way to explore the physical mechanism in optical systems for the enhancement of light–matter interaction, sensing, and detection.

C. Phase modulation

Beyond the amplitude type MEMS devices, nano-kirigami structures have exhibited unique capability of phase modulation. As shown in Fig. 5(c), the phase delay of light can be controlled by designing the

out-of-plane deformation of the structure through changing the precursor curve angle,⁵⁷ with which the nano-kirigami patterns of different morphologies can reach different deformation heights (Δh) under the same voltage. By designing eight spiral antennas with phase difference from 0 to 2π , as shown in Fig. 5(d), a gradient phase changing diagram can be obtained, providing an ideal scheme for optical holograms. Moreover, it was found that a fractal nano-kirigami structure can convert the spin angular momentum into orbital angular momentum to generate the optical vortex (OV) beam,⁵⁸ as illustrated in Fig. 5(e). Compared with traditional metasurface-based phase modulation devices, the nano-kirigami devices could achieve pixelated phase modulation and also utilize a single structure to generate OV beam without multiple structural configuration. Therefore, the phase modulation capability of nano-kirigami structures provides a convenient and efficient platform for the customized operation of the light field beyond the geometrical optics employed in conventional micromirror devices.

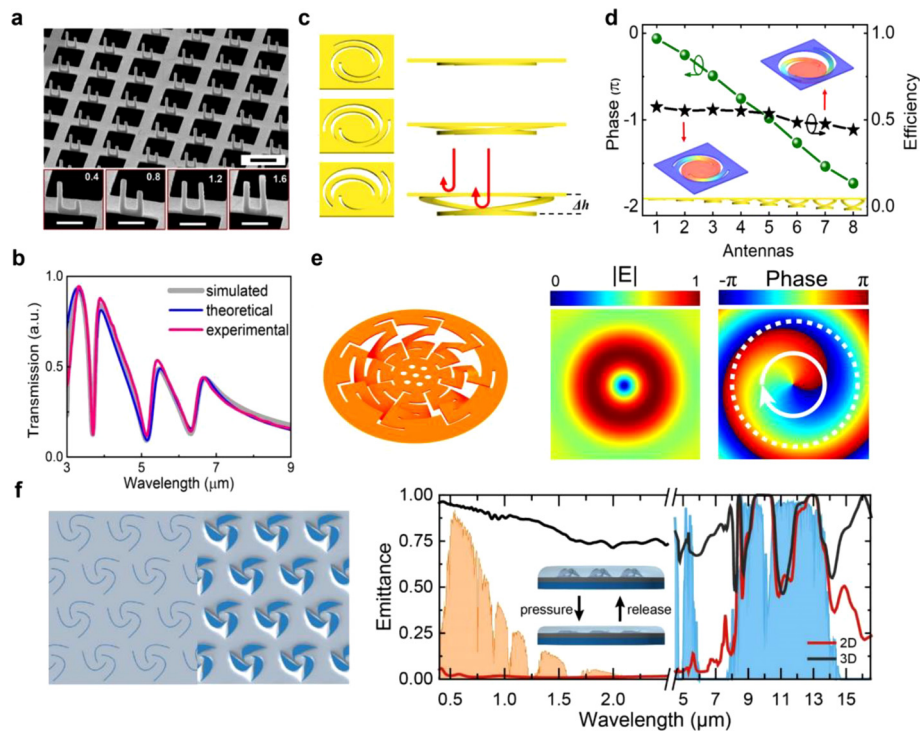


FIG. 5. Applications in Fano resonance generation, phase modulation, and thermal management. (a) SEM images of aSRRs with different arm lengths fabricated by FIB.⁵⁵ Scale bars : $2\ \mu\text{m}$ (Insets: $1\ \mu\text{m}$). (b) Simulated, theoretical, and experimental transmission spectra of the array in (a), which show excellent agreement on Fano resonances.⁵⁵ (c) Side-view and front-view images of three kinds of 3D deformed spiral structures with different azimuth angles under the same bias voltage.⁵⁷ (d) Phase retardation and reflection efficiency of eight spiral units.⁵⁷ (e) Simulated optical vortex (OV) distributions of a deformable fractal nano-kirigami structure.⁵⁸ (f) Visible and infrared emittance spectra of the pinwheel structures with PDMS framework and silicon substrate in 2D and 3D state.⁶² The orange and blue shades are the solar spectral and atmospheric window, respectively. (a) and (b) Reproduced with permission from Liu *et al.*, *Sci. Rep.* **7**(1), 8010 (2017). Copyright 2017 Springer Nature.⁵⁵ (c) and (d) Reproduced with permission from Han *et al.*, *Opt. Express* **29**(19), 30751–30760 (2021). Copyright 2021 Optica Publishing Group.⁵⁷ (e) Reproduced with permission from Hong *et al.*, *Adv. Opt. Mater.* **11** (1), 2202150 (2023). Copyright 2023 Wiley.⁵⁸ (f) Reproduced with permission from Zhao *et al.*, *Small* **20**(3), 2305171 (2024). Copyright 2024 Wiley.⁶²

D. Thermal management

The deformable ability of the nano-kirigami structures also found applications in thermal management. In recent years, researchers have made great progress on regulating the static properties of thermal radiation, such as spectral distribution, directionality, and polarization.^{59–61} However, the dynamic modulation of thermal radiation is still challenging. To address this issue, we proposed a thermal radiation modulation platform with multi-dimensional regulation based on nano-kirigami metasurface.⁶² As shown in Fig. 5(f), a polymer-embedded nano-kirigami thermal management device can be used by dynamically adjusting the absorption and emission of light across visible to infrared wavelengths by mechanical pressing. In the visible wavelengths, the pinwheel structure works like a window that dynamically reflects or receives solar energy. With the increase in deformation height, the window area continues to increase, leading to increased visible light transmission and absorption. In the infrared wavelengths, the structures can dynamically modulate the peak wavelength and intensity of thermal radiation based on the principle of radiative cooling. With the advantages of multi-physics field regulation, multi-dimensional optical property modulation, and multi-material compatibility, such reconfigurable thermal radiation modulation system is expected to play an important role in the fields of energy conversion and thermal camouflage, compared

with the thermal emission manipulation devices fabricated by conventional fabrication methods.

E. Reconfigurable optoelectronic devices

Considering most devices fabricated by traditional 3D micro-/nanofabrication are irreversible, we further developed a reconfigurable nano-kirigami configuration based on FIB-etching and electrostatic forces.³⁵ As shown in Fig. 6(a), a 2D pinwheel array is fabricated by FIB or EBL lithography and the subsequent wet etching process. When a proper voltage is applied, the pinwheel array deforms downward under the attraction of electrostatic force. Within the range of elastic limit, the maximum modulation rate can reach 91% at $\lambda = 1860\ \text{nm}$. More importantly, this high-contrast modulation is experimentally reversible, which strongly proves the feasibility of the electromechanically reconfigurable strategy.

Moreover, to achieve the pixelated structural modulation, a reprogrammable metasurface was designed in which the structural deformations and associated phase delays of each pixel can be independently controlled.⁵⁷ As illustrated in Fig. 6(b), dynamic switching between different holographic images was realized by applying different voltages to each pixel. Such light manipulation ability is highly

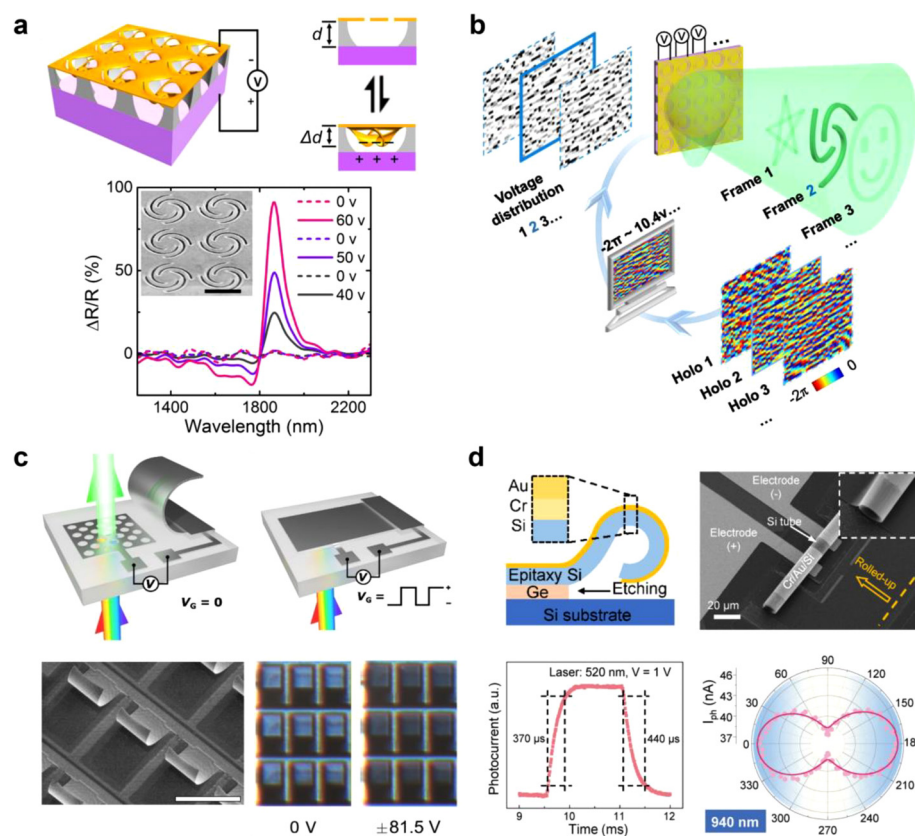


FIG. 6. Reconfigurable optoelectronic applications. (a) Schematic of reconfigurable nano-kirigami by electrostatic force and dynamic modulation contrast of nano-kirigami under DC voltage.³⁵ Scale bar: 1 μm . (b) Pixelated voltage-controllable nano-kirigami patterns for holographic displays.⁵⁷ (c) Schematic of color display device based on co-modulation of plasmonic nanohole array and cantilever.⁶⁵ Scale bar: 50 μm . (d) Device fabrication, photoresponse performance, and polarization detection characteristics of self-rolled-up Si microtubular photodetectors.¹⁸ (a) Reproduced with permission from Chen *et al.*, Nat. Commun. **12**(1), 1299 (2021). Copyright 2021 Springer Nature.³⁵ (b) Reproduced with permission from Han *et al.*, Opt. Express **29**(19), 30751–30760 (2021). Copyright 2021 OSA.⁵⁷ (c) Reproduced with permission from Han *et al.*, Sci. Adv. **8**, eabn0889 (2022). Copyright 2022 AAAS.⁶⁵ (d) Reproduced with permission from Wu *et al.*, Adv. Mater. **35**, 2306715 (2023). Copyright 2023 Wiley.¹⁸

desirable for 3D displays, data storage systems, digital projectors, maskless photolithography, etc.

Rollled-up nanomembranes is another ingenious kirigami like method that can transform specific 2D precursor structures into micro/nano tubular devices.^{63,64} For example, as plotted in Fig. 6(c), Han *et al.* combined the plasmonic metasurfaces and MEMS technology and realized a full-range electrical controlled RGB color display.⁶⁵ In Fig. 6(d), Wu *et al.* also proposed a nondestructive release and crimp process to fabricate tubular photodetectors based on freestanding single-crystalline Si nanomembranes,¹⁸ in which the microtubule structure exhibits significantly polarimetric angle-dependent light absorption.

IV. CONCLUSIONS AND OUTLOOKS

In conclusion, 3D nano-kirigami/origami technology has enabled substantial progresses on nanofabrication methods and optical applications. A number of exotic fabrication methods and geometric configurations have emerged in the fields of mechanics, microelectronics, acoustics, and optics. Versatile 2D-to-3D transformation stimuli methods, such as capillary forces, residual stress, mechanical stress, and FIB irradiation-induced stress, have been explored and brought out interesting applications in the field of nanophotonics and optoelectronic devices. Despite the inspirational progresses, both opportunities and challenges co-exist in this emerging area, including further developments in structural design, material usage, multi-physics field driving methods, and reprogrammable devices, as presented later.

A. Design methods

Most existing nano-kirigami/origami designs are derived from the experience in nature and life that are limited by intuitive thinking and imagination. From the perspective of structural topology, these nano-kirigami/origami structures are mostly tree-type and close-loop structures,³⁰ which are still simple compared to the diverse functional and performance requirements in application scenarios. Moreover, the design of nano-kirigami/origami is relatively decentralized, and a systematic and scientific model has not yet been formed. Finally, powerful inverse design methods^{66,67} that can quickly predict the target 3D geometries and the on-demand external excitation forms/magnitudes have not been explored in micro/nanoscale.⁶⁸ In this regard, combining theoretical models with optimization algorithms to establish inverse design strategies for target geometries can greatly extend and optimize nano-kirigami/origami designs, which may further inspire innovative physics and applications.

B. Innovative materials

Realization of nano-kirigami/origami structures in emerging material platforms is highly promising. One advantage of nano-kirigami/origami is the compatibility of a wide range of materials. Currently, the nano-kirigami scheme has been applied on gold, silver, aluminum, silicon nitride, and phase-change materials, which can be further promoted by adopting other material platforms such as 2D materials. For example, Liu *et al.* developed a high-precision

technique to sculpt extremely precise patterns in 2D materials.⁶⁹ Wang *et al.* proposed a graphene origami/kirigami method to realize the spiral growth of graphene multilayer films.⁷⁰ The combination of the unique morphology of nano-kirigami/origami and the excellent physical properties of 2D materials is expected to have foreseeable applications in the fields of micro/nano-optoelectronic devices and semiconductors.

C. Multi-physics field driving

Currently, most of the nano-kirigami dynamic modulations were achieved by single physics field, such as mechanical, optical, and electric actuations.^{32,35,36} On the one hand, the mechanisms of thermal, magnetic, and acoustic driving still remain at the theoretical stage and need further experimental verification, although some magnetic/acoustic-driven kirigami^{37,71} in millimeter scale set up good templates for future investigation. On the other hand, the couplings among multi-physics fields could trigger more profound light-matter interactions and reconfiguration mechanisms, which will be helpful to create functional nanostructures with exceptional performances. Moreover, the above research works relied on *in situ* nano-kirigami/origami reconfigurable deformation, in which these nano-kirigami structures cannot be detached from the substrate and move freely in 3D space for other applications. For example, optical tweezers can capture and manipulate nanoparticles and biological cells by constructing optical potential wells through laser convergence.^{72–74} If the freely moveable nano-kirigami can be manipulated by light, it will attribute the structures with additional freedom of movement, providing more possibilities for the applications in nanorobotics, microfluidics, bio-sensing, chiral separation in medicine, etc.

D. Reprogrammable devices

The dynamic modulation of optical fields has been of great significance based on reconfiguration schemes, such as electrical bias,^{75,76} mechanical strain,⁷⁷ thermal effects,⁷⁸ liquid crystals,⁷⁹ and phase-change materials.^{80,81} In particular, spatial light modulation in conjunction with conventional MEMS/NEMS shows promising applications.⁸² Therefore, it is expected that the pixelated electromechanical reprogrammable metasurface scheme could provide a useful solution for the development of tunable optoelectronic devices. However, the high-resolution, multi-pixel, dynamically addressable, and high-frequency response nano-kirigami devices have not yet been realized. It is necessary to further optimize 3D micro/nanofabrication technology to ensure high-quality precursor production and precise pixelated nano-kirigami fabrication. In addition, it is also critical to design patterns with large deformation through numerical simulation and topological morphology mechanism. At last, researchers should strengthen cooperation with fields such as semiconductors and integrated circuits, which will further promote the industrialization process of nano-kirigami technology.

ACKNOWLEDGMENTS

This work was supported by the National Natural Science Foundation of China (Grant Nos. T2325005 and 62375016) and the Science and Technology Project of Guangdong (No. 2020B010190001). The authors thank the Analysis and Testing Center from BIT for assistance in facility support.

AUTHOR DECLARATIONS

Conflict of Interest

The authors have no conflicts to disclose.

Author Contributions

Yingying Chen: Data curation (equal); Investigation (lead); Writing – original draft (lead); Writing – review & editing (equal). **Xiaowei Li:** Supervision (supporting). **Lan Jiang:** Supervision (supporting). **Yang Wang:** Writing – review & editing (equal). **Jiafang Li:** Supervision (lead); Writing – review & editing (equal).

DATA AVAILABILITY

The data that support the findings of this study are available from the corresponding author upon reasonable request.

REFERENCES

- Z. Wang, L. Jing, K. Yao, Y. Yang, B. Zheng, C. M. Soukoulis, H. Chen, and Y. Liu, *Adv. Mater.* **29**(27), 1700412 (2017).
- J. Rogers, Y. Huang, O. G. Schmidt, and D. H. Gracias, *MRS Bull.* **41**(2), 123–129 (2016).
- A. Lamoureux, K. Lee, M. Shlian, S. R. Forrest, and M. Shtein, *Nat. Commun.* **6**(1), 8092 (2015).
- J. L. Silverberg, A. A. Evans, L. McLeod, R. C. Hayward, T. Hull, C. D. Santangelo, and I. Cohen, *Science* **345**(6197), 647–650 (2014).
- S. A. Zirbel, R. J. Lang, M. W. Thomson, D. A. Sigel, P. E. Walkemeyer, B. P. Trease, S. P. Magleby, and L. L. Howell, *J. Mech. Des.* **135**(11), 111005 (2013).
- J. Deng, H. Ji, C. Yan, J. Zhang, W. Si, S. Baunack, S. Oswald, Y. Mei, and O. G. Schmidt, *Angew. Chem., Int. Ed.* **52**(8), 2326–2330 (2013).
- K. Kuribayashi, K. Tsuchiya, Z. You, D. Tomus, M. Umamoto, T. Ito, and M. Sasaki, *Mater. Sci. Eng., A* **419**(1), 131–137 (2006).
- Y. Yang, K. Vella, and D. P. Holmes, *Sci. Rob.* **6**(54), eabd6426 (2021).
- A. K. Brooks, S. Chakravarty, M. Ali, and V. K. Yadavalli, *Adv. Mater.* **34**(18), 2109550 (2022).
- H. Luan, Q. Zhang, T.-L. Liu, X. Wang, S. Zhao, H. Wang, S. Yao, Y. Xue, J. W. Kwak, W. Bai, Y. Xu, M. Han, K. Li, Z. Li, X. Ni, J. Ye, D. Choi, Q. Yang, J.-H. Kim, S. Li, S. Chen, C. Wu, D. Lu, J.-K. Chang, Z. Xie, Y. Huang, and J. A. Rogers, *Sci. Adv.* **7**(43), eabj3686 (2021).
- X. Cheng, Z. Fan, S. Yao, T. Jin, Z. Lv, Y. Lan, R. Bo, Y. Chen, F. Zhang, Z. Shen, H. Wan, Y. Huang, and Y. Zhang, *Science* **379**(6638), 1225–1232 (2023).
- Y. Zhang, Z. Yan, K. Nan, D. Xiao, Y. Liu, H. Luan, H. Fu, X. Wang, Q. Yang, J. Wang, W. Ren, H. Si, F. Liu, L. Yang, H. Li, J. Wang, X. Guo, H. Luo, L. Wang, Y. Huang, and J. A. Rogers, *Proc. Natl. Acad. Sci. U. S. A.* **112**(38), 11757–11764 (2015).
- S. Xu, Z. Yan, K.-I. Jang, W. Huang, H. Fu, J. Kim, Z. Wei, M. Flavin, J. McCracken, R. Wang, A. Badea, Y. Liu, D. Xiao, G. Zhou, J. Lee, H. U. Chung, H. Cheng, W. Ren, A. Banks, X. Li, U. Paik, R. G. Nuzzo, Y. Huang, Y. Zhang, and J. A. Rogers, *Science* **347**(6218), 154–159 (2015).
- Z. Tian, B. Xu, G. Wan, X. Han, Z. Di, Z. Chen, and Y. Mei, *Nat. Commun.* **12**(1), 509 (2021).
- Q. Liu, Y. Chen, Z. Feng, Z. Shu, and H. Duan, *Natl. Sci. Rev.* **9**(11), nwab231 (2022).
- D. Xia and J. Notte, *Adv. Mater. Interfaces* **9**(28), 2200696 (2022).
- K. Wang, C. Hou, L. Cong, W. Zhang, L. Fan, X. Wang, and L. Dong, *Small Methods* **7**(7), 2201627 (2023).
- B. Wu, Z. Zhang, Z. Zheng, T. Cai, C. You, C. Liu, X. Li, Y. Wang, J. Wang, H. Li, E. Song, J. Cui, G. Huang, and Y. Mei, *Adv. Mater.* **35**(52), 2306715 (2023).
- S. Chen, J. Chen, X. Zhang, Z.-Y. Li, and J. Li, *Light* **9**(1), 75 (2020).
- R. R. A. Syms, E. M. Yeatman, V. M. Bright, and G. M. Whitesides, *J. Microelectromech. Syst.* **12**(4), 387–417 (2003).
- J.-H. Cho, M. D. Keung, N. Verellen, L. Lagae, V. V. Moshchalkov, P. Van Dorpe, and D. H. Gracias, *Small* **7**(14), 1943–1948 (2011).
- S. Pandey, M. Ewing, A. Kunas, N. Nguyen, D. H. Gracias, and G. Menon, *Proc. Natl. Acad. Sci. U. S. A.* **108**(50), 19885–19890 (2011).

- ²³O. G. Schmidt and K. Eberl, *Nature* **410**(6825), 168–168 (2001).
- ²⁴X. Li, *Adv. Opt. Photonics* **3**(4), 366–387 (2011).
- ²⁵M. K. Blees, A. W. Barnard, P. A. Rose, S. P. Roberts, K. L. McGill, P. Y. Huang, A. R. Ruyack, J. W. Kevek, B. Kobrin, D. A. Muller, and P. L. McEuen, *Nature* **524**(7564), 204–207 (2015).
- ²⁶W. Liu, Q. Zou, C. Zheng, and C. Jin, *ACS Nano* **13**(1), 440–448 (2019).
- ²⁷A. Cui, Z. Liu, J. Li, T. H. Shen, X. Xia, Z. Li, Z. Gong, H. Li, B. Wang, J. Li, H. Yang, W. Li, and C. Gu, *Light* **4**(7), e308 (2015).
- ²⁸L. Xia, W. Wu, J. Xu, Y. Hao, and M. S. Wang, *19th IEEE International Conference on Micro Electro Mechanical Systems*, (IEEE, 2006), pp. 118–121.
- ²⁹K. Chalapat, N. Chekurov, H. Jiang, J. Li, B. Parviz, and G. S. Paraoanu, *Adv. Mater.* **25**(1), 91–95 (2013).
- ³⁰Z. Liu, H. Du, J. Li, L. Lu, Z.-Y. Li, and N. X. Fang, *Sci. Adv.* **4**(7), eaat4436 (2018).
- ³¹J. Li and Z. Liu, *Nanophotonics* **7**(10), 1637–1650 (2018).
- ³²S. Chen, W. Wei, Z. Liu, X. Liu, S. Feng, H. Guo, and J. Li, *Photonics Res.* **8**(7), 1177–1182 (2020).
- ³³Y. Chen, Q. Liang, C.-Y. Ji, X. Liu, R. Wang, and J. Li, *J. Appl. Phys.* **131**(23), 233102 (2022).
- ³⁴Y. Zhao, C.-Y. Ji, H. Yang, Y. Wang, H. Xie, and J. Li, *J. Opt.* **24**, 054007 (2022).
- ³⁵S. Chen, Z. Liu, H. Du, C. Tang, C.-Y. Ji, B. Quan, R. Pan, L. Yang, X. Li, C. Gu, X. Zhang, Y. Yao, J. Li, N. X. Fang, and J. Li, *Nat. Commun.* **12**(1), 1299 (2021).
- ³⁶L. Zhiguang, H. Du, Z.-Y. Li, N. Fang, and J. Li, *APL Photonics* **3**, 100803 (2018).
- ³⁷P. Cao, W. Ou, Y. Su, Y. Yuhang, E. Dong, Z. Song, J. Li, and Y. Zhang, *Phys. Rev. Appl.* **18**, 054040 (2022).
- ³⁸Y. Tang, Z. Liu, J. Deng, K. Li, J. Li, and G. Li, *Laser Photonics Rev.* **14**(7), 2000085 (2020).
- ³⁹Y. Mei, G. Huang, A. A. Solovov, E. B. Ureña, I. Mönch, F. Ding, T. Reindl, R. K. Y. Fu, P. K. Chu, and O. G. Schmidt, *Adv. Mater.* **20**(21), 4085–4090 (2008).
- ⁴⁰Q. Liu, W. Wang, M. F. Reynolds, M. C. Cao, M. Z. Miskin, T. A. Arias, D. A. Muller, P. L. McEuen, and I. Cohen, *Sci. Rob.* **6**(52), eabe6663 (2021).
- ⁴¹T. Yoshida, A. Baba, and T. Asano, *Jpn. J. Appl. Phys., Part 1* **44**(7S), 5744 (2005).
- ⁴²B. C. Park, K. Y. Jung, W. Y. Song, B. H. O, and S. J. Ahn, *Adv. Mater.* **18**(1), 95–98 (2006).
- ⁴³R. Pan, Z. Li, Z. Liu, W. Zhu, L. Zhu, Y. Li, S. Chen, C. Gu, and J. Li, *Laser Photonics Rev.* **14**(1), 1900179 (2020).
- ⁴⁴R. Pan, Z. Liu, W. Zhu, S. Du, C. Gu, and J. Li, *Adv. Funct. Mater.* **31**(31), 2100689 (2021).
- ⁴⁵Y. Han, Z. Liu, S. Chen, J. Liu, Y. Wang, and J. Li, *Photonics Res.* **8**(9), 1506–1511 (2020).
- ⁴⁶L. Zhiguang, Y. Xu, C. Y. Ji, S. Chen, X. Li, X. Zhang, Y. Yao, and J. Li, *Adv. Mater.* **32**, 1907077 (2020).
- ⁴⁷C. Y. Ji, S. Chen, Y. Han, X. Liu, J. Liu, J. Li, and Y. Yao, *Nano Lett.* **21**(16), 6828–6834 (2021).
- ⁴⁸X. Li, C. Y. Ji, S. Chen, Y. Han, J. Liu, and J. Li, *Adv. Opt. Mater.* **9**(24), 2101191 (2021).
- ⁴⁹X. Liu, Q. Liang, X. Zhang, C.-Y. Ji, and J. Li, *Nanophotonics* **12**(8), 1459–1468 (2023).
- ⁵⁰U. Fano, *Phys. Rev.* **124**(6), 1866–1878 (1961).
- ⁵¹B. Luk'yanchuk, N. I. Zheludev, S. A. Maier, N. J. Halas, P. Nordlander, H. Giessen, and C. T. Chong, *Nat. Mater.* **9**(9), 707–715 (2010).
- ⁵²M. Rahmani, B. Luk'yanchuk, and M. Hong, *Laser Photonics Rev.* **7**(3), 329–349 (2013).
- ⁵³Z. Liu, Z. Liu, J. Li, W. Li, J. Li, C. Gu, and Z.-Y. Li, *Sci. Rep.* **6**(1), 27817 (2016).
- ⁵⁴Z. Liu, S. Du, A. Cui, Z. Li, Y. Fan, S. Chen, W. Li, J. Li, and C. Gu, *Adv. Mater.* **29**(17), 1606298 (2017).
- ⁵⁵Z. Liu, J. Li, Z. Liu, W. Li, J. Li, C. Gu, and Z.-Y. Li, *Sci. Rep.* **7**(1), 8010 (2017).
- ⁵⁶X. Tian, Z. Liu, H. Lin, B. Jia, Z. Y. Li, and J. Li, *Nanoscale* **10**(35), 16630–16637 (2018).
- ⁵⁷Y. Han, S. Chen, C. Ji, X. Liu, Y. Wang, J. Liu, and J. Li, *Opt. Express* **29**(19), 30751–30760 (2021).
- ⁵⁸X. Hong, Q. Liang, X. Liu, C.-Y. Ji, and J. Li, *Adv. Opt. Mater.* **11**(1), 2202150 (2023).
- ⁵⁹T. Mori, Y. Yamauchi, S. Honda, and H. Maki, *Nano Lett.* **14**(6), 3277–3283 (2014).
- ⁶⁰T. Inoue, M. De Zoysa, T. Asano, and S. Noda, *Nat. Mater.* **13**(10), 928–931 (2014).
- ⁶¹D. G. Baranov, Y. Xiao, I. A. Nechipurenko, A. Krasnok, A. Alù, and M. A. Kats, *Nat. Mater.* **18**(9), 920–930 (2019).
- ⁶²Y. Zhao, Q. Liang, S. Li, Y. Chen, X. Liu, H. Sun, C. Wang, C.-Y. Ji, J. Li, and Y. Wang, *Small* **20**(3), 2305171 (2024).
- ⁶³X. Cheng and Y. Zhang, *Adv. Mater.* **31**(36), 1901895 (2019).
- ⁶⁴B. Wu, Z. Zhang, C. Wang, E. Song, J. Cui, G. Huang, P. Zhou, Z. Di, and Y. Mei, *Appl. Phys. Lett.* **121**(6), 060503 (2022).
- ⁶⁵Z. Han, C. Frydendahl, N. Mazurski, and U. Levy, *Sci. Adv.* **8**(16), eabn0889 (2022).
- ⁶⁶Z. Fan, Y. Yang, F. Zhang, Z. Xu, H. Zhao, T. Wang, H. Song, Y. Huang, J. A. Rogers, and Y. Zhang, *Adv. Mater.* **32**(14), 1908424 (2020).
- ⁶⁷Y. Bai, H. Wang, Y. Xue, Y. Pan, J.-T. Kim, X. Ni, T.-L. Liu, Y. Yang, M. Han, Y. Huang, J. A. Rogers, and X. Ni, *Nature* **609**(7928), 701–708 (2022).
- ⁶⁸R. Bo, S. Xu, Y. Yang, and Y. Zhang, *Chem. Rev.* **123**(18), 11137–11189 (2023).
- ⁶⁹X. Liu, S. T. Howell, A. Conde-Rubio, G. Boero, and J. Brugger, *Adv. Mater.* **32**(31), 2001232 (2020).
- ⁷⁰Z.-J. Wang, X. Kong, Y. Huang, J. Li, L. Bao, K. Cao, Y. Hu, J. Cai, L. Wang, H. Chen, Y. Wu, Y. Zhang, F. Pang, Z. Cheng, P. Babor, M. Kolibal, Z. Liu, Y. Chen, Q. Zhang, Y. Cui, K. Liu, H. Yang, X. Bao, H.-J. Gao, Z. Liu, W. Ji, F. Ding, and M.-G. Willinger, *Nat. Mater.* **23**(3), 331–338 (2024).
- ⁷¹X. Kuang, S. Wu, Q. Ze, L. Yue, Y. Jin, S. M. Montgomery, F. Yang, H. J. Qi, and R. Zhao, *Adv. Mater.* **33**(30), 2102113 (2021).
- ⁷²P. S. Kolipara, X. Li, J. Li, Z. Chen, H. Ding, Y. Kim, S. Huang, Z. Qin, and Y. Zheng, *Nat. Commun.* **14**(1), 5133 (2023).
- ⁷³J. Li, E. H. Hill, L. Lin, and Y. Zheng, *ACS Nano* **13**(4), 3783–3795 (2019).
- ⁷⁴J. Li, P. S. Kolipara, Y. Liu, K. Yao, Y. Liu, and Y. Zheng, *ACS Nano* **16**(6), 8820–8826 (2022).
- ⁷⁵J. Li, P. Yu, S. Zhang, and N. Liu, *Nat. Commun.* **11**(1), 3574 (2020).
- ⁷⁶B. Zeng, Z. Huang, A. Singh, Y. Yao, A. K. Azad, A. D. Mohite, A. J. Taylor, D. R. Smith, and H.-T. Chen, *Light* **7**(1), 51 (2018).
- ⁷⁷S. C. Malek, H.-S. Ee, and R. Agarwal, *Nano Lett.* **17**(6), 3641–3645 (2017).
- ⁷⁸A. Komar, R. Paniagua-Domínguez, A. Miroshnichenko, Y. F. Yu, Y. S. Kivshar, A. I. Kuznetsov, and D. Neshev, *ACS Photonics* **5**(5), 1742–1748 (2018).
- ⁷⁹C. Zou, A. Komar, S. Fasold, J. Bohn, A. A. Muravsky, A. A. Murauski, T. Pertsch, D. N. Neshev, and I. Staude, *ACS Photonics* **6**(6), 1533–1540 (2019).
- ⁸⁰S. Abdollahramezani, O. Hemmatyar, M. Taghinejad, H. Taghinejad, Y. Kiarashinejad, M. Zandehshahvar, T. Fan, S. Deshmukh, A. A. Eftekhari, W. Cai, E. Pop, M. A. El-Sayed, and A. Adibi, *Nano Lett.* **21**(3), 1238–1245 (2021).
- ⁸¹X. Li, C. Cao, C. Liu, W. He, K. Wu, Y. Wang, B. Xu, Z. Tian, E. Song, J. Cui, G. Huang, C. Zheng, Z. Di, X. Cao, and Y. Mei, *Nat. Commun.* **13**(1), 7819 (2022).
- ⁸²L. Cong, P. Pitchappa, C. Lee, and R. Singh, *Adv. Mater.* **29**(26), 1700733 (2017).